Diode Laser Spectrum of OCS: The ν_1 Band at 2062 cm^{-1}

W. Klebsch, Koichi Yamada, and G. Winnewisser

I. Physikalisches Institut, Universität zu Köln

Z. Naturforsch. **38a**, 157–162 (1983); received December 16, 1982

Dedicated to Professor Alfred Klemm on the occasion of his 70th birthday

The ν_1 band of OCS has been measured in the wavenumber range 2026 to 2081 cm^{-1} to an accuracy better than 0.0008 cm^{-1} using a diode laser spectrometer. The width of the observed lines is essentially Doppler-limited. The observed lines could be assigned to the following hot bands: 11^10-01^10, 12^00-02^00, 12^20-02^20, 10^01-00^01, 11^11-01^11 of OCS and to 10^00-00^00 and 11^10-01^10 of the isotopic species $OC^{34}S$ and $OC^{33}S$ in natural abundances. These data provide a secondary standard in this wavelength region.

I. Introduction

The precise measurements of high resolution spectra obtained with tunable diode lasers are intrinsically connected with the problem of having highly accurate calibration spectra available. Stable, light linear molecules such as OCS serve as convenient wavenumber calibration standards. Recently Maki and coworkers [1, 2, 3] measured for this purpose infrared spectra of the 859 cm^{-1}-, 1050 cm^{-1}- and 1711 cm^{-1}-bands of OCS with high resolution by combination of grating and tunable diode laser spectroscopy. In the present work we have investigated the ν_1 band, centered at 2062 cm^{-1}, for similar reasons, with a tunable diode laser spectrometer.

This band had been measured previously by Meyer-Bourbonneux and Meyer [4] and Blanquet et al. [5] by SISAM-spectrometers with a resolution of 0.03 to 0.05 cm^{-1}. The former observed the fundamental bands of $OC^{32}S$, $OC^{34}S$ and $OC^{33}S$ and one hot band arising from the 01^10 state of $OC^{32}S$. Blanquet et al. used a ^{34}S enriched sample, and investigated the fundamental and hot band arising from the 01^10 state of both isotopic species $OC^{34}S$ and $O^{13}C^{34}S$. However their data lack the accuracy required for calibration sjpectra.

Guelachvili [6] measured with very high precision the ν_1-fundamental band of OCS using a large FT spectrometer. However no satellite spectra were reported such as hot bands or bands arising from isotopic species, which are particularly helpful in providing a sufficiently dense calibration spectrum.

Reprint requests to W. Klebsch, I. Physikal. Institut der Universität zu Köln, Universitätsstr. 14, 5000 Köln 41.

There is usually one additional difficulty associated with providing calibration spectra, which is connected with the narrow tuning range of a single laser mode (typically ~ 1 cm^{-1}). For proper identification of the calibration lines in diode laser spectra it is essential to recognize the spectral pattern and to know the detailed features of the spectrum. Therefore in the present work we assigned and measured a few hot bands of OCS and bands arising from $OC^{34}S$ and $OC^{33}S$ in natural abundance. These new measurements together with the FT-measurements of Guelachvili now serve as calibration standards.

The numbering of normal modes are defined in this paper as follows:

ν_1 = stretching mode of higher frequency,

ν_2 = bending mode, and

ν_3 = stretching mode of lower frequency.

This definition agrees with Mulliken's recommendation [7] and Herzberg's definition [8], but is different from most previous publications on OCS, where ν_1 and ν_3 are interchanged.

II. Experimental

The rovibrational spectra of OCS were measured in the 2030–2100 cm^{-1} region by a tunable diode laser in our laboratory. The details of the spectrometer are given elsewhere [9, 10]. The source frequency was modulated by 5 kHz sine wave and the signal was demodulated at 10 kHz by lock-in amplifiers.

The cell used in the present work is a 60 cm long pyrex glass tube of 3 cm inner diameter. Both ends

0340-4811 / 83 / 0200-0157 $ 01.3 0/0. – Please order a reprint rather than making your own copy.

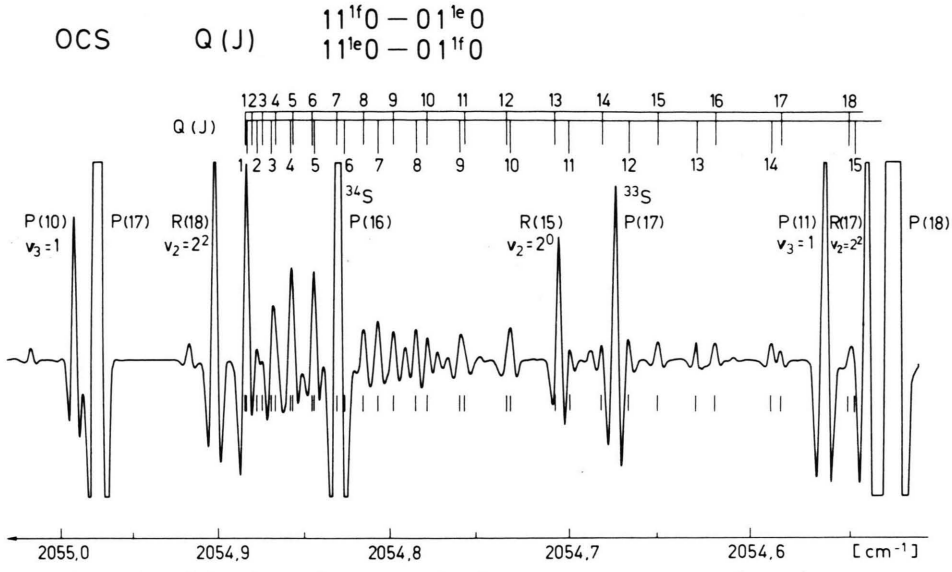

Fig. 1. A portion of the observed spectrum showing the Q branch of the 11^10-01^10 band near 2055 cm^{-1}.

of the cell were sealed by BaF_2 windows. Since the ν_1 band is very strong, the sample gas pressure in the cell was always less than 100 Pa. Thus the effect of pressure broadening on the line width was negligible compared to contributions from the Doppler width.

The wavenumbers of the observed lines were calibrated by using Guelachvili's data for the fundamental band. At the high frequency end of the band no data are available from Guelachvili and thus the CO lines were used for calibration [11]. The precision of the present measurements is better than 0.0008 cm^{-1}.

A portion of the measured spectrum near 2054 cm^{-1} is shown in second derivative form in Fig. 1, recorded at room temperature.

Although the spectrum is dominated by strong P and R branch transitions arising from various vibrational states and isotopic species, including those from $OC^{33}S$ in natural abundance (0.76%), its most prominent feature is the weak 11^10-01^10 Q branch, whose lines show l-type splitting commencing already at $J=3$. The J assignment of these Q branch transitions rests on the P and R branch lines measured and identified in this work.

The sensitivity of the spectrometer was sufficient to measure the R(101) transition of the fundamental band of OCS with a good S/N ratio at room temperature.

III. Assignments and Analysis

Since the spacing between the adjacent J transitions of the fundamental band is not strongly dependent on J and the accuracy of our wavenumber measurement using Ge-etalon fringes is not good enough, it is difficult to identify the J assignment of the fundamental band only from the spacing. In some cases we measured the OCS spectra together with CO spectra to confirm the identification. A Loomis-Wood diagram was then made to extend the assignment. The diagram shows the relative positions of satellite bands, and smooth changes in the positions of satellite bands prove that the identification is correct. By trial-and-error method, we obtained consistent assignments for a number of short pieces of spectra measured by the diode laser spectrometer. Then the analysis of the transition wavenumbers for the satellite lines was straight forward. We used a least squares program based on the conventional expressions,

$$E(J) = G_v + B_{v(\alpha)}(J(J+1) - l^2) - D_{v(\alpha)}(J(J+1) - l^2)^2 + H_{v(\alpha)}(J(J+1) - l^2)^3, \quad (1)$$

$$\nu(J' - J'') = E'(J') - E''(J''), \quad (2)$$

and

$$\nu_0 = G'_v - G''_v, \quad (3)$$

where α means e or f when the l-degeneracy is resolved [12].

The identification of the band and the assignments of J quantum numbers were performed with the help of microwave data [1, 2, 13–18] in the lower states. The iteration process described in [9] was successfully applied.

We have identified the following transitions for the normal species:

(a) $10^00 - 00^00$ P(71) – R(101)
(b) $11^10 - 01^10$ P(57) – R(91), Q(1) – Q(18)
(c) $12^00 - 02^00$ P(37) – R(53)
(d) $12^20 - 02^20$ P(35) – R(48), Q(2) – Q(21)
(e) $10^01 - 00^01$ P(65) – R(84)
(f) $11^11 - 01^11$ R(8) – R(26)

for the $OC^{34}S$ species

(g) $10^00 - 00^00$ P(62) – R(100)
(h) $11^10 - 01^10$ P(57) – R(54)

and for the $OC^{33}S$ species

(i) $10^00 - 00^00$ P(50) – R(74)
(j) $11^10 - 01^10$ R(8) – R(36).

The Q branches were observed for two bands, (b) and (d). They served as an exact test of the assignment.

For the $\Pi - \Pi$ hot bands the obtained constants are effective values for the l-doubling components. Since the energy correction for the l-type doubling is

$$\Delta E = \pm \tfrac{1}{2} (q_v J(J+1) + q_J J^2 (J+1)^2), \quad (4)$$

the l-type doubling constants q_v and q_J are obtained by

$$q_v = (B_{v(f)} - B_{v(e)})$$

and

$$q_J = (D_{v(f)} - D_{v(e)}). \quad (5)$$

The rotational and centrifugal distortion constants for the $l = 1$ states are then

$$B_v = (B_{v(e)} + B_{v(f)})/2 \quad (6)$$

and

$$D_v = (D_{v(e)} + D_{v(f)})/2 .$$

Table 1. Spectroscopic Parameters obtained for the ν_1 band of OCS (in cm^{-1})*.

Band	10^00-00^00	11^10-01^10	10^01-00^01	
	2062.20127 (a)	2054.88483 (8)	2059.13892 (10)	
B'	0.201641413 (a)	0.20201509 (12)	0.20110097 (19)	
B''	0.202856754 (b)	0.2032098606 (c)	0.202251835 (d)	
D'	0.044034 (a)	0.044590 (43)	0.049245 (74)	$\times 10^{-6}$
D''	0.043423 (b)	0.044150 (c)	0.044277 (c)	$\times 10^{-6}$
H'	0.0318 (a)	0.0118 (37)	0.2445 (74)	$\times 10^{-12}$
H''	0.0 (a)	0.0 (fixed)	0.0 (fixed)	$\times 10^{-12}$
q' (v)		0.21531 (24)		$\times 10^{-3}$
q'' (v)		0.212135 (c)		$\times 10^{-3}$
$q'(J)$		−0.219 (86)		$\times 10^{-9}$
$q''(J)$		−0.010 (c)		$\times 10^{-9}$
$q'(JJ)$		5.1 (74)		$\times 10^{-15}$
$q''(JJ)$		0.0 (c)		$\times 10^{-15}$
Band	12^20-02^20	12^00-02^00	11^11-01^11	
	2047.61073 (12)	2048.51308 (11)	2051.68111 (58)	
B'	0.20238405 (26)	0.20231045 (21)	0.20150784 (37)	
B''	0.203559474 (c)	0.203480476 (c)	0.20265751 (e)	
D'	0.04966 (11)	0.038006 (75)		$\times 10^{-6}$
D''	0.048634 (c)	0.036572 (c)		$\times 10^{-6}$
q' (v)			0.23547 (93)	$\times 10^{-6}$
q'' (v)			0.22860 (e)	$\times 10^{-6}$

* The numbers in parentheses are one standard deviation obtained in the present analysis and the letters give the references for the constants which were fixed in the analysis as follows: a = Ref. [6], b = Ref. [13], c = Ref. [14], d = Ref. [15], e = Ref. [1].

For the Δ states, we could not resolve the e and f components. Thus the constants are directly obtained by (1).

The introduction of the last term in (1) was found to be necessary for the fundamental bands of OCS, $OC^{34}S$ and $OC^{33}S$, where high J transitions were included in the fit. For the $\Pi-\Pi$ hot band (b) of $OC^{32}S$ we could determine the H constants both from e and f species. They are identical within one standard deviation.

IV. Results and Discussion

The rovibrational parameters, such as ν_0, B_v, D_v, H_v, q_v and q_J, were determined for the $v_1 = 1$ state and combination states related to $v_2 = 1$ for OCS, $OC^{34}S$ and $OC^{33}S$ as listed in Table 1, 2 and 3. The

Table 2. Spectroscopic Parameters obtained for $OC^{34}S$ (in cm^{-1})*.

Band	10^00-00^00	11^10-01^10	
	2061.44564(8)	2054.13041(6)	
B'	0.19671577(12)	0.19707989(17)	
B''	0.1978980333(f)	0.198242592(g, h)	
D'	0.041982(35)	0.042351(57)	$\times10^{-6}$
D''	0.0414046(f)	0.041830(g)	$\times10^{-6}$
H'	0.0252(25)		$\times10^{-12}$
H''	0.0(fixed)		$\times10^{-12}$
$q'(v)$		0.20491(33)	$\times10^{-3}$
$q''(v)$		0.20243345(h)	$\times10^{-3}$
$q'(J)$		−0.083(114)	$\times10^{-9}$
$q''(J)$		−0.1310(b)	$\times10^{-9}$

* See footnote of Table 1: f = Ref. [2]; g = Ref. [16]; h = Ref. [17].

Table 3. Spectroscopic Parameters obtained for $OC^{33}S$ (in cm^{-1})*.

Band	10^00-00^00	11^10-01^10	
	2061.80878(9)	2054.49233(20)	
B'	0.19910371(12)	0.19947282(10)	
B''	0.2003024509(k)	0.206511036(k)	
D'	0.042770(23)	0.04350(x)	$\times10^{-6}$
D''	0.0423869(k)	0.043066827(k)	$\times10^{-6}$
$q'(v)$		0.20899(20)	$\times10^{-3}$
$q''(v)$		0.20714097(k)	$\times10^{-3}$
$q'(J)$		−0.237(x)	$\times10^{-9}$
$q''(J)$		−0.1348(k)	$\times10^{-9}$

* See footnote of Table 1. k = Ref. [18]; x = Assumed value (mean value of corresponding D's for ^{32}S and ^{34}S).

Table 4. Transition wavenumbers for the 11^10-01^10 band of OCS.

$J'-J''$	e − e calculated	o − c	f − f calculated	o − c
59 − 60	2026.3129		2026.2961	
58 − 59	2026.8586		2026.8420	
57 − 58	2027.4020		2027.3856	
56 − 57	2027.9431	−0.0011	2027.9269	−0.0009
55 − 56	2028.4818		2028.4658	
54 − 55	2029.0181		2029.0024	
53 − 54	2029.5521		2029.5366	
52 − 53	2030.0838		2030.0685	
51 − 52	2030.6131		2030.5981	
50 − 51	2031.1401		2031.1253	
49 − 50	2031.6648		2031.6501	
48 − 49	2032.1870	−0.0006	2032.1726	−0.0006
47 − 48	2032.7070	0.0009	2032.6928	0.0000
46 − 47	2033.2246		2033.2106	
45 − 46	2033.7398		2033.7260	
44 − 45	2034.2527		2034.2392	
43 − 44	2034.7632		2034.7499	
42 − 43	2035.2714		2035.2583	
41 − 42	2035.7773		2035.7644	
40 − 41	2036.2807	0.0002	2036.2681	0.0007
39 − 40	2036.7819	−0.0008	2036.7694	−0.0002
38 − 39	2037.2806		2037.2684	
37 − 38	2037.7771		2037.7651	
36 − 37	2038.2711		2038.2594	
35 − 36	2038.7628	0.0001	2038.7513	0.0001
34 − 35	2039.2521	0.0000	2039.2409	−0.0004
33 − 34	2039.7391		2039.7281	
32 − 33	2040.2237		2040.2130	
31 − 32	2040.7060		2040.6955	
30 − 31	2041.1859		2041.1756	
29 − 30	2041.6634		2041.6534	
28 − 29	2042.1386		2042.1289	
27 − 28	2042.6114		2042.6019	
26 − 27	2043.0818		2043.0726	
25 − 26	2043.5499	−0.0001	2043.5410	−0.0005
24 − 25	2044.0156		2044.0069	
23 − 24	2044.4789	0.0004	2044.4706	−0.0001
22 − 23	2044.9399		2044.9318	
21 − 22	2045.3985		2045.3907	
20 − 21	2045.8547	−0.0002	2045.8472	0.0001
19 − 20	2046.3085	0.0004	2046.3014	0.0005
18 − 19	2046.7600	0.0000	2046.7532	0.0001
17 − 18	2047.2091	0.0005	2047.2026	0.0002
16 − 17	2047.6558	0.0004	2047.6496	−0.0003
15 − 16	2048.1002	0.0004	2048.0943	0.0000
14 − 15	2048.5422	−0.0002	2048.5366	−0.0002
13 − 14	2048.9818		2048.9766	
12 − 13	2049.4190		2049.4141	
11 − 12	2049.8538		2049.8493	

Table 4. Continued

$J'-J''$	e – e calculated	o – c	f – f calculated	o – c
10 – 11	2050.2863		2050.2821	
9 – 10	2050.7164		2050.7126	
8 – 9	2051.1441	0.0013	2051.1406	0.0006
7 – 8	2051.5694	0.0007	2051.5663	−0.0002
6 – 7	2051.9923	−0.0005	2051.9896	−0.0004
5 – 6	2052.4128	0.0005	2052.4106	−0.0013
4 – 5	2052.8310		2052.8291	
3 – 4	2053.2468		2053.2453	
2 – 3	2053.6601		2053.6590	
1 – 2	2054.0711		2054.0705	
2 – 1	2055.6912	−0.0007	2055.6922	
3 – 2	2056.0902	0.0009	2056.0917	−0.0006
4 – 3	2056.4868		2056.4888	
5 – 4	2056.8811		2056.8834	
6 – 5	2057.2729		2057.2757	
7 – 6	2057.6623	−0.0001	2057.6656	0.0014
8 – 7	2058.0494	−0.0006	2058.0532	0.0004
9 – 8	2058.4340	−0.0008	2058.4383	−0.0003
10 – 9	2058.8162	0.0008	2058.8210	0.0007
11 – 10	2059.1961	−0.0015	2059.2013	−0.0009
12 – 11	2059.5735	0.0010	2059.5792	0.0009
13 – 12	2059.9485	0.0000	2059.9547	−0.0001
14 – 13	2060.3211	−0.0003	2060.3279	0.0001
15 – 14	2060.6913	0.0005	2060.6986	0.0004
16 – 15	2061.0591	−0.0001	2061.0669	0.0001
17 – 16	2061.4245	0.0001	2061.4328	0.0000
18 – 17	2061.7875	−0.0008	2061.7963	
19 – 18	2062.1480	0.0000	2062.1574	−0.0004
20 – 19	2062.5062	0.0000	2062.5161	0.0000
21 – 20	2062.8619	0.0001	2062.8724	0.0001
22 – 21	2063.2152		2063.2262	
23 – 22	2063.5661		2063.5777	
24 – 23	2063.9146		2063.9267	−0.0015
25 – 24	2064.2606	−0.0017	2064.2733	
26 – 25	2064.6042	−0.0003	2064.6175	
27 – 26	2064.9454		2064.9593	
28 – 27	2065.2842		2065.2987	
29 – 28	2065.6206		2065.6356	
30 – 29	2065.9545	−0.0006	2065.9701	−0.0001
31 – 30	2066.2860	0.0009	2066.3022	0.0011
32 – 31	2066.6151	−0.0004	2066.6319	0.0000
33 – 32	2066.9417	0.0001	2066.9592	0.0001
34 – 33	2067.2659	−0.0002	2067.2840	−0.0001
35 – 34	2067.5877	0.0006	2067.6064	00003
36 – 35	2067.9071		2067.9263	
37 – 36	2068.2240		2068.2438	
38 – 37	2068.5385	0.0007	2068.5589	0.0002
39 – 38	2068.8505	−0.0007	2068.8716	0.0005
40 – 39	2069.1601	−0.0006	2069.1818	0.0000
41 – 40	2069.4672	−0.0007	2069.4896	−0.0009

Table 4. Continued

$J'-J''$	e – e calculated	o – c	f – f calculated	o – c
42 – 41	2069.7719	−0.0001	2069.7949	0.0001
43 – 42	2070.0742	0.0000	2070.0978	0.0003
44 – 43	2070.3740	0.0005	2070.3983	−0.0004
45 – 44	2070.6714	0.0000	2070.6963	−0.0010
46 – 45	2070.9664		2070.9918	
47 – 46	2071.2588	0.0003	2071.2850	0.0016
48 – 47	2071.5489		2071.5756	0.0006
49 – 48	2071.8365	0.0007	2071.8638	0.0007
50 – 49	2072.1216	0.0002	2072.1496	0.0005
51 – 50	2072.4043	0.0002	2072.4329	0.0001
52 – 51	2072.6845	0.0009	2072.7138	0.0004
53 – 52	2072.9622		2072.9922	
54 – 53	2073.2375		2073.2681	
55 – 54	2073.5104	0.0000	2073.5416	−0.0005
56 – 55	2073.7808	−0.0010	2073.8126	−0.0016
57 – 56	2074.0487	−0.0018	2074.0811	−0.0011
58 – 57	2074.3142	−0.0003	2074.3472	−0.0006
59 – 58	2074.5772	−0.0005	2074.6109	0.0004
60 – 59	2074.8377	−0.0002	2074.8720	−0.0002
61 – 60	2075.0958	−0.0004	2075.1307	−0.0004
62 – 61	2075.3514	−0.0001	2075.3869	−0.0003
63 – 62	2075.6045	−0.0004	2075.6407	−0.0004
64 – 63	2075.8552	0.0000	2075.8920	0.0008
65 – 64	2076.1034	0.0018	2076.1408	
66 – 65	2076.3491	0.0010	2076.3871	0.0011
67 – 66	2076.5923	0.0012	2076.6309	0.0008
68 – 67	2076.8331	0.0002	2076.8723	0.0007
69 – 68	2077.0714	0.0009	2077.1112	0.0016
70 – 69	2077.3072	0.0017	2077.3476	
71 – 70	2077.5405	0.0000	2077.5815	−0.0004
72 – 71	2077.7714		2077.8129	
73 – 72	2077.9997		2078.0419	
74 – 73	2078.2256		2078.2684	
75 – 74	2078.4490		2078.4923	
76 – 75	2078.6699		2078.7138	
77 – 76	2078.8884		2078.9328	
78 – 77	2079.1043		2079.1493	
79 – 78	2079.3178		2079.3633	
80 – 79	2079.5287		2079.5748	
81 – 80	2079.7372	−0.0011	2079.7839	−0.0010
82 – 81	2079.9432	−0.0010	2079.9904	0.0000
83 – 82	2080.1467	−0.0011	2080.1944	
84 – 83	2080.3477	−0.0008	2080.3959	−0.0004
85 – 84	2080.5462	−0.0007	2080.5949	−0.0006
86 – 85	2080.7422		2080.7915	
87 – 86	2080.9357		2080.9855	0.0001
88 – 87	2081.1267	0.0008	2081.1770	0.0005
89 – 88	2081.3152	−0.0004	2081.3660	−0.0001
90 – 89	2081.5012	0.0003	2081.5525	−0.0003
91 – 90	2081.6847	0.0004	2081.7365	0.0005

rotational parameters of the molecules in lower states were fixed at the values obtained previously by various authors, as listed in the foot notes of the tables.

Although we could extend the measurements of the fundamental band of OCS up to $J = 101$, we could not improve the constants reported by Guelachvili [6]. For the other bands our constants are more precise than those of earlier work and some of them were newly determined.

Recently Bogey and Bauer [19] have measured the microwave spectra of OCS in highly excited vibrational states. Their constants for 11^10 and 10^01 states of OCS and 10^00 state of $OC^{34}S$ are in very good agreement with the present data. The accuracy of the constants in these states determined in the present work is slightly better, because we have measured a large number of transitions with high J and analysed the data with the centrifugal distortion correction terms.

In Table 4 we present the measured and calculated wave numbers for the 11^10-01^10 band of OCS which are intended to be used together with Guelachvili's data [6] as calibration standards. Additional listings of the observed OCS spectra will be available from the authors upon request.

Acknowledgement

This work was supported in part by grants given through the Deutsche Forschungsgemeinschaft SFB-131-Radioastronomie.

[1] A. G. Maki, W. B. Olson, and R. L. Sams, J. Mol. Spectrosc. **81,** 122 (1980).
[2] J. S. Wells, F. R. Petersen, A. G. Maki, and D. J. Sukle, J. Mol. Spectrosc. **89,** 421 (1981).
[3] J. P. Sattler, T. L. Worchesky, A. G. Maki, and W. J. Lafferty, J. Mol. Spectrosc. **90,** 460 (1981).
[4] F. Meyer-Bourbonneux and C. Meyer, C. R. Acad. Sci. Paris B, 1224 (1970).
[5] G. Blanquet, J. Walrand, and C. P. Courtoy, J. Mol. Spectrosc. **81,** 473 (1980).
[6] G. Guelachvili, Opt. Commun. **30,** 361 (1979).
[7] R. S. Mulliken, J. Chem. Phys. **23,** 1997 (1955).
[8] G. Herzberg, Molecular Spectra and Molecular Structure, Vol. II, D. van Nostrand Comp., Toronto 1968.
[9] K. Yamada, R. Schieder, G. Winnewisser, and A. W. Mantz, Z. Naturforsch. **35 a,** 690 (1980).
[10] K. Yamada and G. Winnewisser, Z. Naturforsch. **36 a,** 23 (1981).
[11] G. Guelachvili, J. Mol. Spectrosc. **75,** 251 (1979).
[12] J. M. Brown, J. T. Hougen, K.-P. Huber, J. W. C. Johns, I. Kopp, H. Levebvre-Brion, A. J. Merer, D. A. Ramsay, J. Rostas, and R. N. Zare, J. Mol. Spectrosc. **55,** 500 (1975).
[13] A. G. Maki, J. Phys. Chem. Ref. Data **3,** 221 (1974).
[14] N. W. Larsen and B. P. Winnewisser, Z. Naturforsch. **29 a,** 1213 (1974).
[15] M. Sergent-Rozey and Ngyen van Than, Infrared Physics **21,** 221 (1981).
[16] J. G. Smith, J. Chem. Soc. Faraday Trans. II, **72,** 2298 (1976).
[17] J. M. L. J. Reinartz, W. L. Meerts, and A. Dymanus, Chem. Phys. Lett. **16,** 576 (1972).
[18] A. V. Burenin, A. N. Val'dov, E. N. Karyakin, A. F. Krupnov, and S. M. Shapin, J. Mol. Spectrosc. **87,** 312 (1981).
[19] M. Bogey and A. Bauer, J. Mol. Spectrosc. **84,** 170 (1980).